iScience

CellPress
OPEN ACCESS

Article

YAP/TAZ Are Required to Suppress Osteogenic Differentiation of Vascular Smooth Muscle Cells

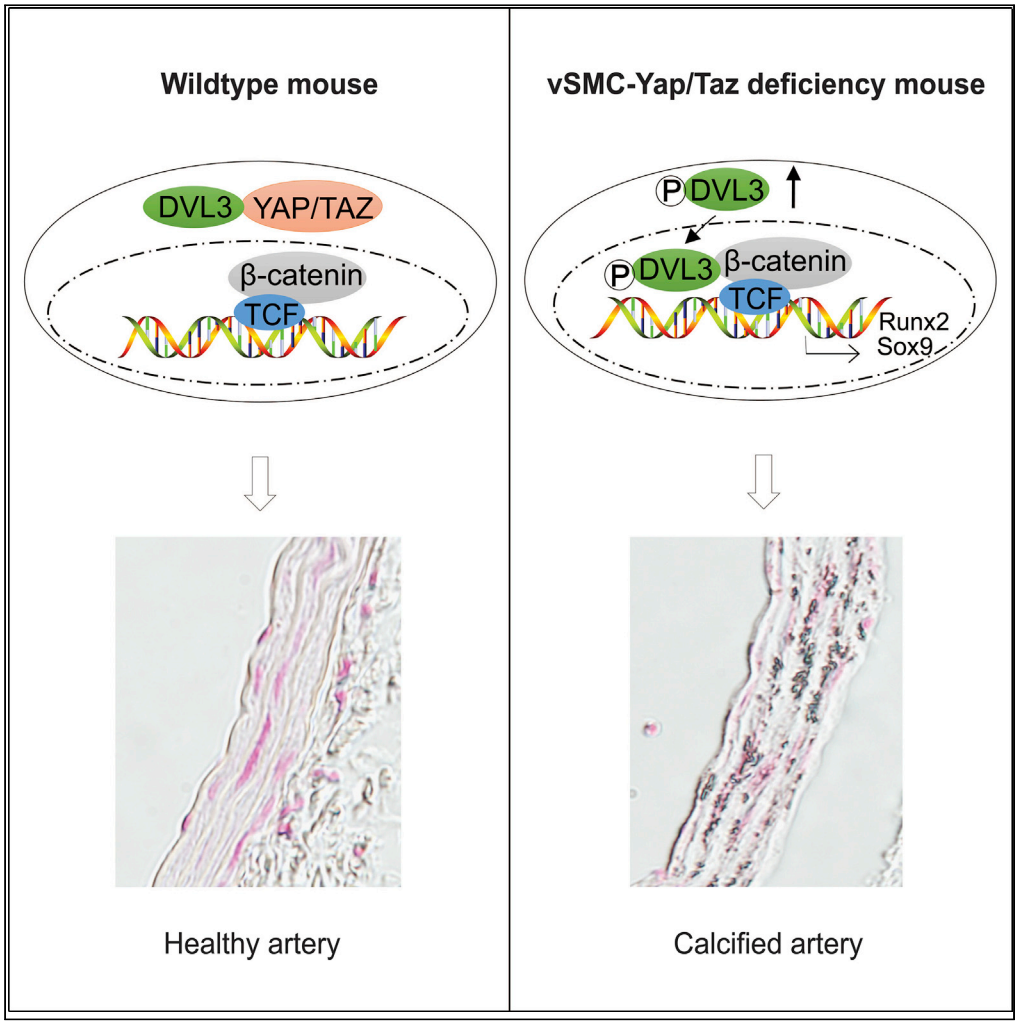

Lei Wang, Ramesh Chennupati, Young-June Jin, Rui Li, ShengPeng Wang, Stefan Günther, Stefan Offermanns

lei.wang@mpi-bn.mpg.de (L.W.)
stefan.offermanns@mpi-bn.mpg.de (S.O.)

HIGHLIGHTS

YAP/TAZ play an important role in maintaining vascular SMCs contractile phenotype

Loss of YAP/TAZ in vSMCs leads to reduced expression of smooth muscle marker genes

Loss of YAP/TAZ in vSMCs results in reduced artery contractility

Deficiency of YAP/TAZ in vSMCs leads to osteogenic transdifferentiation

Wang et al., iScience *23*, 101860
December 18, 2020
https://doi.org/10.1016/j.isci.2020.101860

iScience

CellPress
OPEN ACCESS

Article

YAP/TAZ Are Required to Suppress Osteogenic Differentiation of Vascular Smooth Muscle Cells

Lei Wang,[1,*] Ramesh Chennupati,[1] Young-June Jin,[1] Rui Li,[1] ShengPeng Wang,[1,2] Stefan Günther,[3] and Stefan Offermanns[1,4,5,6,*]

SUMMARY

Vascular smooth muscle cells (VSMCs) represent the prevailing cell type of arterial vessels and are essential for blood vessel structure and homeostasis. They have substantial potential for phenotypic plasticity when exposed to various stimuli in their local microenvironment. How VSMCs maintain their differentiated contractile phenotype is still poorly understood. Here we demonstrate that the Hippo pathway effectors YAP and TAZ play a critical role in maintaining the differentiated contractile phenotype of VSMCs. In the absence of YAP/TAZ, VSMCs lose their differentiated phenotype and undergo osteogenic differentiation, which results in vascular calcification. Osteogenic transdifferentiation was accompanied by the upregulation of Wnt target genes. The absence of YAP/TAZ in VSMCs led to Disheveled 3 (DVL3) nuclear translocation and upregulation of osteogenesis-associated genes independent of canonical Wnt/β-catenin signaling activation. Our data indicate that cytoplasmic YAP/TAZ interact with DVL3 to avoid its nuclear translocation and osteogenic differentiation, thereby maintaining the differentiated phenotype of VSMCs.

INTRODUCTION

Vascular smooth muscle cells (VSMCs) are the predominant cell type of the arterial vessel wall and play an essential role in the structure and function of the blood vessel. They have substantial potential for phenotypic plasticity when exposed to particular stimuli in their local microenvironment (Bennett et al., 2016; Owens et al., 2004). Differentiated, quiescent VSMCs express a range of marker genes, such as smooth muscle myosin heavy-chain (MYH11), 22-kDa SMC lineage-restricted protein (SM22α/TAGLN) or smooth muscle actin (ACTA2). When kept in culture or after vascular injury, expression of these marker genes decreases, and expression of non-muscle MHC and other genes such as c-fos, Egr-1, and epiregulin increases, indicating VSMC dedifferentiation (Miano, 2010; Owens et al., 2004; Sobue et al., 1999; Takahashi et al., 2003). Under pathological conditions, VSMCs can also transdifferentiate and acquire a macrophage-like phenotype characterized by the expression of macrophage markers including CD68 and LGALS3 (Feil et al., 2014; Rong et al., 2003; Shankman et al., 2015; Vengrenyuk et al., 2015) or an osteo-chondrogenic phenotype, which is characterized by expression of particular markers, such as Runx2, Sox9, or Alpl (Durham et al., 2018; Speer et al., 2009; Woldt et al., 2012).

VSMC plasticity is under the control of many regulatory transcriptional pathways (Gomez and Owens, 2012; Kawai-Kowase and Owens, 2007). Two main VSMC transcriptional programs are controlled by the activity of serum response factor (SRF), depending on its interaction with specific co-factors (Posern and Treisman, 2006; Wang et al., 2004). Although co-activators of the myocardin family promote VSMC differentiation, competitive binding of the ternary complex factor (TCF) family of Ets-domain proteins induces decreased expression of smooth muscle marker genes and VSMC proliferation (Mack, 2011). TCFs are phosphorylated and activated through the Ras/MAP-kinase (MAPK) pathway (Posern and Treisman, 2006), whereas RhoA-mediated signaling has been shown to promote nuclear translocation of myocardin-related transcription factors and induce VSMC differentiation (Lu et al., 2001; Mack et al., 2001; Olson and Nordheim, 2010). Recent evidence shows that the transdifferentiation of VSMCs toward a macrophage-like phenotype is regulated by Kruppel-like factor 4 (KLF4) (Shankman et al., 2015). Osteo-chondrogenic differentiation of VSMCs is believed to be responsible for vascular calcification, which was found in advanced atherosclerotic lesions as well as in type-2 diabetes, chronic kidney disease, and aged patients (Abedin et al., 2004; Vattikuti and Towler, 2004). Several signaling pathways promoting osteo-chondrogenic differentiation of VSMCs have been described. Among these is the Wnt/β-catenin pathway, which has been shown to

[1]Max Planck Institute for Heart and Lung Research, Department of Pharmacology, Bad Nauheim 61231, Germany

[2]Cardiovascular Research Center, School of Basic Medical Sciences, Xi'an Jiaotong University Health Science Center, Yanta District, Xi'an 710061, China

[3]Bioinformatics and Deep Sequencing Platform, Max Planck Institute for Heart and Lung Research, Bad Nauheim 61231, Germany

[4]Center for Molecular Medicine, Medical Faculty, Goethe University, Frankfurt am Main 60590, Germany

[5]German Center for Cardiovascular Research (DZHK), Partner Site Frankfurt Rhine-Main, 13347 Berlin, Germany

[6]Lead Contact

*Correspondence: lei.wang@mpi-bn.mpg.de (L.W.), stefan.offermanns@mpi-bn.mpg.de (S.O.)

https://doi.org/10.1016/j.isci.2020.101860

modulate Runx2 expression (Cai et al., 2016; Rong et al., 2014; Shalhoub et al., 2006; Yao et al., 2015). Evidence has also provided that osteogenic differentiation of VSMCs can be induced by activation of the bone morphogenetic protein (BMP)/SMAD pathway (Nakagawa et al., 2010; Zhu et al., 2015) as well as by the NF-κB signaling pathway (Voelkl et al., 2018; Yoshida et al., 2017; Zhao et al., 2012). However, the relative role of these signaling pathways and their regulation as well as the mechanisms preventing spontaneous transdifferentiation of VSMCs *in vivo* are poorly understood.

YAP and TAZ are cellular co-factors and effectors of the Hippo signaling pathway, which regulate various cellular processes, including cell proliferation, cell differentiation, and cell survival by integrating different cellular signaling pathways (Koo and Guan, 2018; Ma et al., 2019; Panciera et al., 2017; Totaro et al., 2018). YAP/TAZ exert their effects by co-activation or co-repression of gene expression in the nucleus (Lin et al., 2017; Zheng and Pan, 2019) as well as by interaction with cytoplasmic proteins in a transcriptionally independent manner (Azzolin et al., 2014; Barry et al., 2013; Gao et al., 2015; Varelas et al., 2010). In VSMCs, expression of YAP has been shown to increase in response to vascular injury (Wang et al., 2012; Xie et al., 2012; Yu et al., 2019), and overexpression of YAP or activation of YAP/TAZ by thromboxane A_2 *in vitro* promotes VSMC proliferation (Feng et al., 2016; Wang et al., 2012; Xie et al., 2012). Loss or suppression of YAP expression *in vitro* and *in vivo* results in the increased expression of smooth muscle marker genes and in attenuated injury-induced smooth muscle phenotype switch and neointima formation (Wang et al., 2012; Xie et al., 2012). This indicates a role of YAP in injury-induced VSMC dedifferentiation. However, the role of both YAP and TAZ, which in most cells have redundant functions (Reginensi et al., 2015; Sakabe et al., 2017; Xin et al., 2013), in VSMCs of normal mature arteries is not known.

Here we show that cytoplasmic YAP and TAZ inhibit nuclear translocation of DVL3, Wnt target gene expression, and osteogenic transdifferentiation of VSMCs to maintain their differentiated contractile phenotype.

RESULTS

VSMCs Lose Their Differentiated Contractile Phenotype in the Absence of YAP and TAZ

To study the function of YAP and TAZ in vascular smooth muscle cells, we generated inducible smooth muscle-specific YAP- and TAZ-deficient mice by crossing mice carrying floxed alleles of Yap and Taz ($Yap^{fl/fl}$; $Taz^{fl/fl}$) with the Myh11-$CreER^{T2}$ mouse line (Wirth et al., 2008). Smooth muscle-specific tamoxifen-induced YAP/TAZ-deficient mice (Myh11-$CreER^{T2}$;$Yap^{fl/fl}$;$Taz^{fl/fl}$, hereafter termed: Sm-Yap/Taz-KO) showed strong tamoxifen-induced recombination of both floxed alleles in vascular smooth muscle cells, resulting in loss of YAP and TAZ proteins (Figure 1A). About 2 weeks after the last tamoxifen injection, Sm-Yap/Taz-KO mice started to show abdominal distension as well as signs of apathy and had to be euthanized. At necropsy, the large intestine was distended with feces contents (Figure 1B), indicating large intestinal pseudo-obstruction, most likely due to defective intestinal peristaltic movements, which was also reported while this manuscript was in revision (Daoud et al., 2020). Mice with induced smooth muscle-specific loss of YAP or TAZ alone did not show any signs of intestinal pseudo-obstruction and appeared to be normal (Figures S1A and S1B).

To examine the function of YAP/TAZ in arterial smooth muscle cells, thoracic aortae and femoral arteries were isolated and arterial contractile functions were analyzed by wire myography. The contractile response of arteries from Sm-Yap/Taz-KO mice to phenylephrine and the thromboxane A_2 analogue U46619 was strongly reduced compared with arteries from control animals (Figures 1C, 1D, S1C and S1D). In contrast, mice with smooth muscle-specific loss of YAP or TAZ alone showed no difference (Figures 1C and 1D). Using quantitative RT-PCR (qRT-PCR) analysis, we evaluated the effect of smooth muscle-specific YAP/TAZ deficiency on smooth muscle marker gene expression in the media of arterial vessels and found strongly decreased mRNA levels of α-actin (Acta2), SM22α (Tagln), smooth muscle myosin heavy chain (Myh11), and several other smooth muscle marker genes (Figure 1E). These changes were not observed in the media of arterial vessels from smooth muscle-specific single knockouts of YAP or TAZ (Figure S1E). Reduced expression of smooth muscle marker genes in the media of Sm-Yap/Taz-KO was also seen at the protein level (Figures 1F and 1G). This shows that VSMCs lose their differentiated contractile phenotype after the acute loss of YAP and TAZ *in vivo*.

Loss of YAP/TAZ in VSMCs Leads to Osteogenic Differentiation and Vascular Calcification

To further analyze the consequences of YAP/TAZ deficiency in VSMCs, we measured expression levels of marker genes of smooth muscle de- and trans-differentiation. Although expression of SMemb, a marker gene of the synthetic VSMC phenotype (Owens et al., 2004), was rather reduced (Figure S2), we found that smooth muscle-specific loss of YAP and TAZ resulted in strong upregulation of marker genes indicating osteogenic transdifferentiation

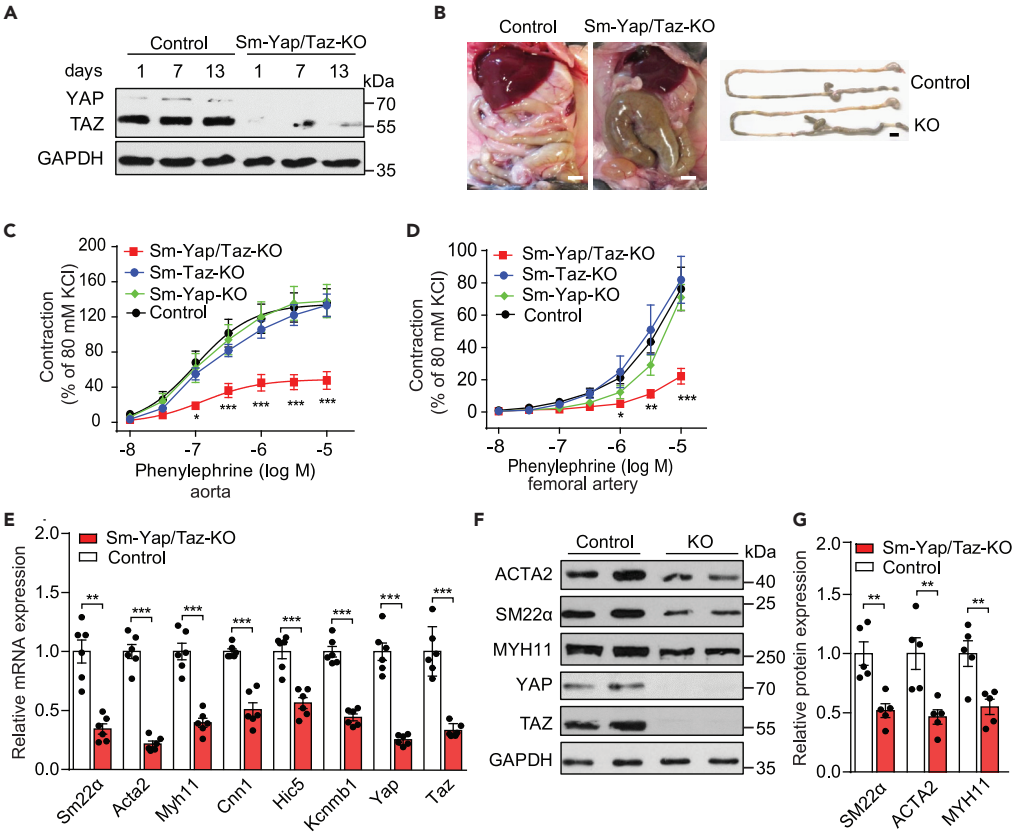

Figure 1. VSMCs Lose Their Differentiated Contractile Phenotype in the Absence of Yap/Taz

(A) Western blot analysis of YAP and TAZ in aortic lysates from control and Sm-Yap/Taz-KO mice at 1, 7, and 13 days after the last tamoxifen injection.

(B) Macroscopic analysis of the gastrointestinal tracts of control and Sm-Yap/Taz-KO (KO) mice. The smooth muscle-specific Yap/Taz knockout mice started to show a dilated, obstructed colon two weeks after the last tamoxifen injection. Scale bar: 1 cm.

(C and D) Contractile responses to phenylephrine of thoracic aortae (n = 6 mice per group (2 experiments per mouse)) (C), femoral arteries (n = 6 mice per group (2 experiments per mouse)) (D).

(E) Quantitative RT-PCR showing mRNA expression of smooth muscle marker genes from mouse aortae two weeks after the last tamoxifen injection (n = 6 mice per group).

(F) Western blot analysis of ACTA2, SM22α, MYH11, YAP, and TAZ expression in aortic lysates from control and Sm-Yap/Taz-KO (KO) mice. One of three representative experiments is shown.

(G) The densitometry analysis of ACTA2, SM22α, and MYH11 from control and Sm-Yap/Taz-KO (KO) mice (n = 5 mice per group).

Data are presented as mean ± SEM. *p < 0.05, **p < 0.01, and ***p < 0.001 (two-way ANOVA in C and D and Student's t test in (E and G)).

such as alkaline phosphatase (Alpl), osteopontin (Spp1), SRY-Box transcription factor 9 (Sox9), and Runt-related transcription factor 2 (Runx2) (Figures 2A and 2B; Table S1). Western blot analysis confirmed the upregulation of ALPL protein levels in the media of Sm-Yap/Taz-KO mice (Figures 2C and 2D). After induction of smooth muscle-specific YAP/TAZ deficiency, we also found a strong increase in the alkaline phosphatase activity in the media of aortae from Sm-Yap/Taz-KO mice (Figure 2E). In addition, von Kossa staining revealed the presence of abnormal calcium deposits in the media of the aortae of Sm-Yap/Taz-KO mice, and we observed an increase in calcium content of the aortae of Sm-Yap/Taz-KO animals (Figures 2F and 2G). These data show that acute loss of vascular smooth muscle cell YAP and TAZ expression results in osteogenic transdifferentiation and vascular calcification.

YAP/TAZ Suppress the Expression of Wnt-Responsive Genes

Several cellular signaling pathways have been shown to regulate osteogenic differentiation of VSMC, including Wnt/β-catenin, NF-κB, Notch and Bmp/Smad signaling (Cai et al., 2016; Hruska et al., 2005;

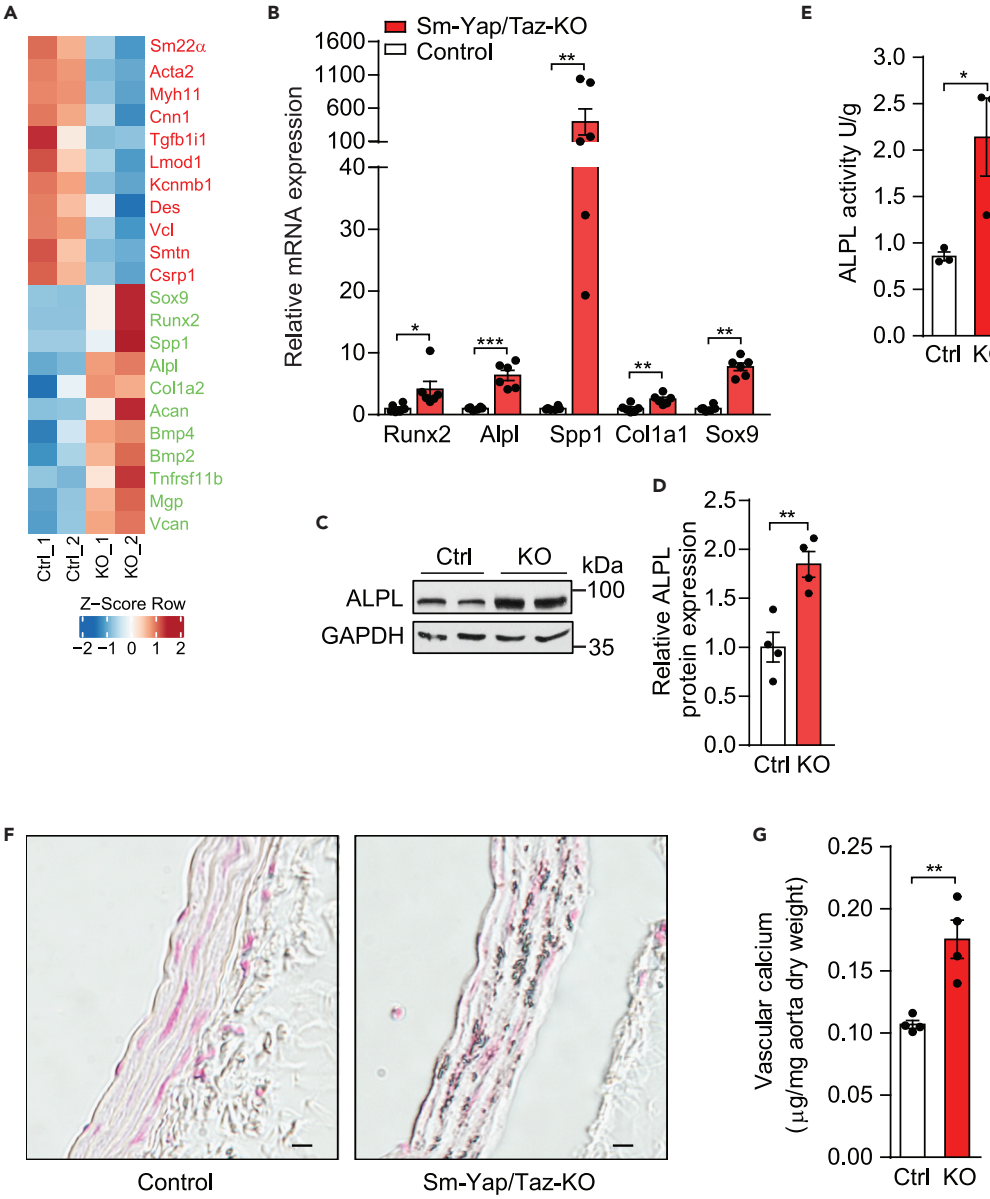

Figure 2. Loss of YAP/TAZ in VSMCs Leads to Osteogenic Differentiation and Vascular Calcification

(A) Heatmap of RNA-seq analysis showing the dysregulated genes in aortic SMC of Sm-Yap/Taz-KO (KO) mice (n = 2 mice per group) two weeks after the last tamoxifen injection, including smooth muscle marker genes (red labels) and osteogenic marker genes (green labels). Ctrl: control.

(B) Quantitative RT-PCR analysis of expression of osteogenic marker genes in aortic SMC of Sm-Yap/Taz-KO mice (n = 6 mice per group).

(C) Western blot analysis of ALPL in aortic SMC lysates from control (Ctrl) and Sm-Yap/Taz-KO (KO) mice two weeks after the last tamoxifen injection. One of three representative experiments is shown.

(D) The bar diagram shows the densitometry analysis of ALPL (n = 4 mice per group).

(E) ALPL enzyme activity assay of aorta from control (Ctrl) and Sm-Yap/Taz-KO (KO) mice two weeks after the last tamoxifen injection (n = 3 mice per group).

(F) Von Kossa staining of descending thoracic aorta from control (Ctrl) and Sm-Yap/Taz-KO mice on day 17 after the last tamoxifen injection. Scale bar: 10 μm.

(G) Calcium content of aorta from control (Ctrl) and Sm-Yap/Taz-KO (KO) mice on day 17 after the last tamoxifen injection (n = 4 mice per group). In C and F one representative experiment of three independent experiments is shown. Data are presented as mean ± SEM. *p < 0.05, **p < 0.01, and ***p < 0.001 (Student's t test in (B, D, E, and G)).

Shao et al., 2005; Shimizu et al., 2009; Voelkl et al., 2018, 2019; Woldt et al., 2012). In aortic VSMCs of Sm-Yap/Taz-KO mice, we did not observe any increase in nuclear β-catenin (Figures 3A and 3B) or in the phosphorylation of P65 or Smad2/3 as well as no change in the level of the Notch intracellular domain (NICD), indicating cleaved Notch (Figure 3C). There was also no increase in nuclear localization of P65 (Figure 3D). This indicates that acute loss of YAP/TAZ in VSMCs does not increase β-catenin, NF-κB, Smad, or Notch signaling. However, when analyzing different target genes, we found an upregulation of Wnt target genes in aortic VSMCs of Sm-Yap/Taz-KO mice (Figures 3E and 3F; Table S1). Thus, loss of YAP/TAZ in VSMCs resulted in increased expression of Wnt-responsive genes but not in β-catenin activation.

YAP/TAZ Bind DVL3 to Prevent Its Nuclear Translocation and Upregulation of Osteogenic Marker Genes in VSMCs

Both immunohistochemical analysis and immunoblotting of fractionated aortic VSMCs revealed that in normal differentiated aortic VSMCs YAP and TAZ reside exclusively in the cytosol but not in the nucleus (Figures 4A and 4B). This strongly suggests that YAP/TAZ prevent osteogenic differentiation of VSMCs through their presence in the cytosol. Because it has been shown that YAP and TAZ can affect Wnt-signaling by cytosolic interaction with Disheveled 1, 2, and 3 (DVL1-3) (Barry et al., 2013; Varelas et al., 2010), we determined their expression and found that DVL3 showed the highest expression of DVL isoforms in VSMCs (Figure 4C). In addition, DVL3 co-precipitated with YAP from lysates of mouse aortic smooth muscle cells (Figure 4D). DVL activity and its localization have been shown to be regulated by phosphorylation indicated by an increased apparent molecular weight upon SDS-PAGE and immunoblot analysis (Gan et al., 2008; Itoh et al., 2005; Wang et al., 2015). We found that a considerable fraction of DVL3 showed reduced mobility in SDS-PAGE analysis when prepared from aortic VSMCs of Sm-Yap/Taz-KO mice compared with control animals (Figure 4E). Consistent with this, a mobility shift of DVL3 prepared from aortic VSMCs of Sm-Yap/Taz-KO mice was also detected on a phos-tag gel (Figure S3). Fractionation of aortic VSMCs revealed that phosphorylated DVL3 found in cells from Sm-Yap/Taz-KO mice localized to the nucleus (Figure 4F). Overexpression of DVL3 carrying a nuclear localization signal (NLS) strongly increased TCF/LEF transcriptional activity as determined by the co-transfection of a TCF/LEF-luciferase reporter construct (Figure 4G). Also, knockdown of YAP/TAZ resulted in increased TCF/LEF-luciferase activity, an effect blocked by suppression of DVL expression (Figure 4H). Because the knockdown of Dvl3 resulted in the upregulation of Dvl2 (Figure S4), we performed a knockdown of all 3 Dvl isoforms. To further characterize the mechanism of increased Wnt target gene expression after loss of YAP/TAZ, we suppressed YAP/TAZ expression in human aortic VSMCs. Knockdown of Yap/Taz expression resulted in increased nuclear localization of DVL3 (Figure 4I) and also led to an increased expression of the Wnt target gene Axin2 and osteogenic marker genes (Figure 4J). This effect was significantly reduced after knockdown of DVL (Figure 4J).

DISCUSSION

Vascular calcification, the deposition of calcium phosphate salts in the arterial wall, occurs in both the intimal and medial layers of arteries (Demer and Tintut, 2008; Lanzer et al., 2014; Sage et al., 2010). Intimal calcification in areas of atherosclerotic plaques is increased by chronic kidney disease, type-2 diabetes mellitus, and aging and is linked to arterial obstruction and atherosclerotic plaque rupture (Sage et al., 2010; Yahagi et al., 2017). In contrast, calcification of the media, which is also promoted by chronic kidney disease, type-2 diabetes, and aging in patients, is linked to vessel stiffness, systolic hypertension, and heart failure (Andrews et al., 2018; Chow and Rabkin, 2015; Nicoll and Henein, 2014). Vascular calcification resembles bone formation and has been recognized as an active process mainly driven by VSMCs (Bostrom, 2000; Durham et al., 2018; Jaminon et al., 2019; Paloian and Giachelli, 2014). The initial mechanisms resulting in vessel calcification may differ between types of vascular calcification, but the osteo-chondrogenic differentiation of VSMCs and the calcification of the media are the central processes underlying the development of calcified vessels (Hortells et al., 2018; Sage et al., 2010; Voelkl et al., 2019). Several signaling pathways have been identified, which promote osteo-chondrogenic differentiation of VSMCs, resulting in vessel calcification (Bartoli-Leonard et al., 2018; Demer and Tintut, 2008; Durham et al., 2018; Shao et al., 2005; Voelkl et al., 2019). Here we show that the Hippo signaling pathway effectors YAP and TAZ suppress osteogenic differentiation of VSMCs in healthy vessels by inhibition of DVL nuclear translocation.

The molecular regulation of osteo-chondrogenic transdifferentiation of VSMCs bears some similarity to that in true bone formation and has been shown to involve BMP and Wnt signaling (Bostrom et al., 2011). The Wnt pathway has in fact been established as a major osteo-inductive signaling pathway in

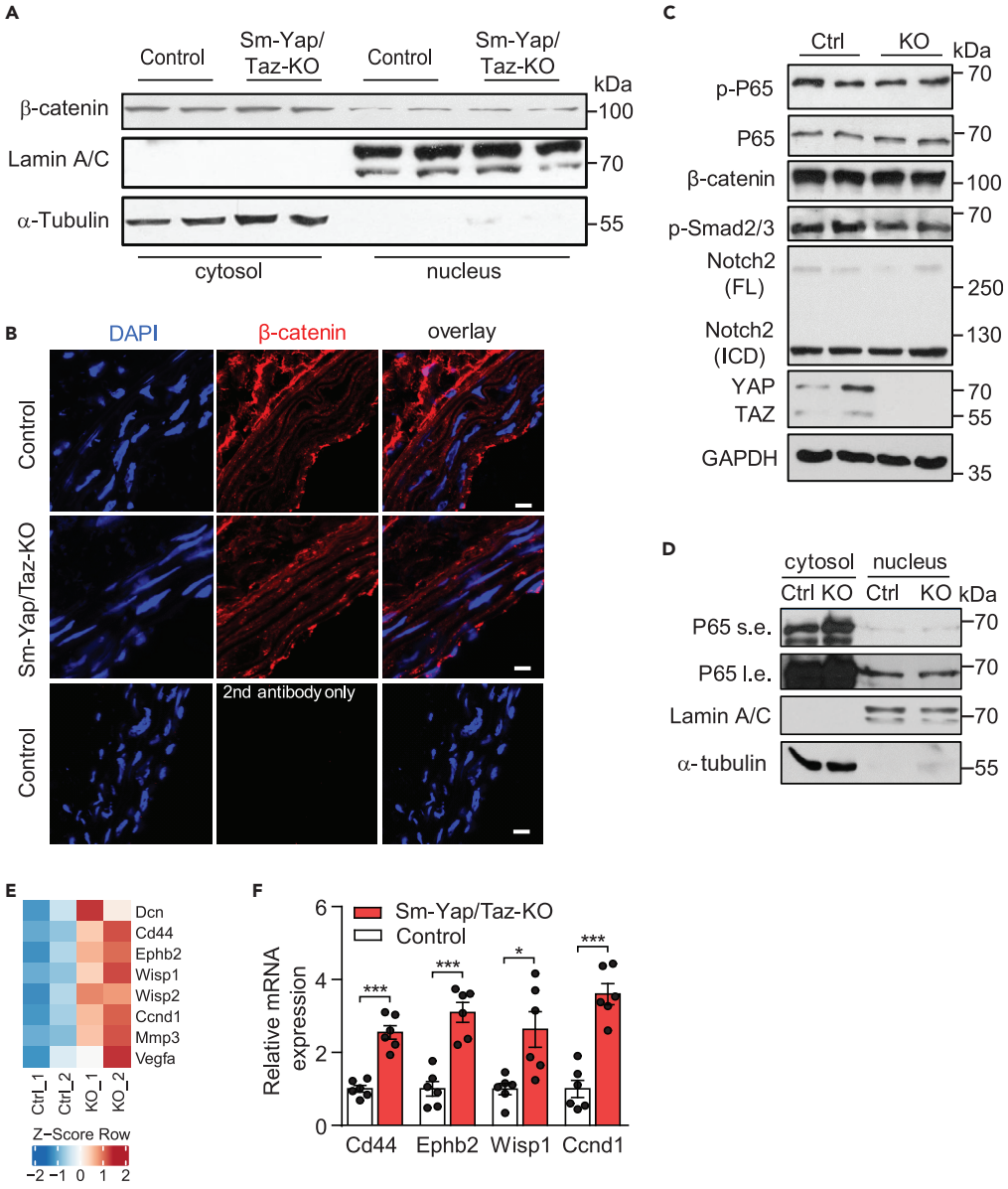

Figure 3. Loss of YAP/TAZ in VSMCs Leads to the Upregulation of Wnt-responsive Genes

(A) Western blot analysis of β-catenin in the cytoplasmic and nuclear fraction of mouse aortic SMC two weeks after the last tamoxifen injection. Lamin A/C was used as a nuclear marker and α-Tubulin as a cytoplasmic marker.

(B) Mouse aorta cross-sections were subjected to immunofluorescence staining with antibody against β-catenin. Scale bar: 10 μm.

(C) Western blot analysis of P65 and phosphorylation of P65 (Ser 536), β-catenin, phosphorylation of Smad2/3, and Notch2 (FL: full-length 300 kDa, ICD: intracellular domain 110 kDa) in the aortic SMC lysates from control and Sm-Yap/Taz-KO (KO) mice two weeks after the last tamoxifen injection.

(D) Western blot analysis of P65 in the cytoplasmic and nuclear fraction of mouse aortic SMC lysates from (Ctrl) and Sm-Yap/Taz-KO (KO). Lamin A/C was used as a nuclear marker and α-tubulin as a cytoplasmic marker. s.e.: short exposure, l.e.: long exposure. In A–D one representative experiment of three independent experiments is shown.

(E) Heatmap of RNA-seq analysis showing upregulated Wnt-responsive genes in aortic SMC of Sm-Yap/Taz-KO (KO) mice (n = 2 mice per group).

(F) Quantitative RT-PCR analysis of expression of several Wnt-responsive genes in the aortic SMC of Sm-Yap/Taz-KO mice two weeks after the last tamoxifen injection (n = 6 mice per group). One of three representative experiments is shown. Data are presented as mean ± SEM. *$p < 0.05$ and **$p < 0.01$ (Student's t test in (F)).

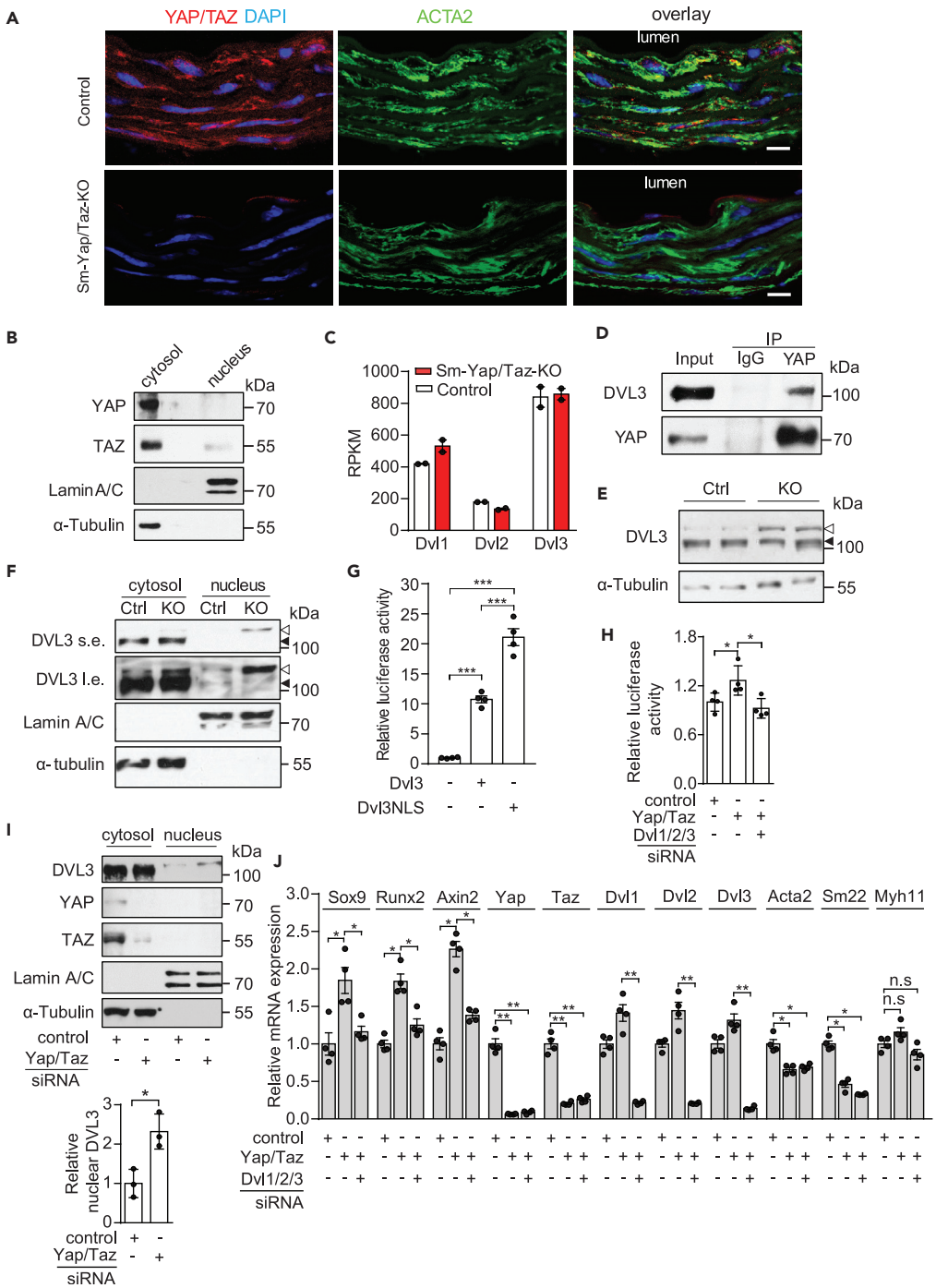

Figure 4. YAP/TAZ Restrict DVL3 Nuclear Translocation

(A) Mouse aorta cross-sections were subjected to immunofluorescence staining with antibodies against YAP/TAZ and ACTA2. Scale bar: 10 μm.

(B) Western blot analysis of YAP/TAZ in the cytoplasmic and nuclear fraction of mouse aortic SMC. Lamin A/C was used as a nuclear marker and α-tubulin as a cytoplasmic marker.

(C) RNA-seq data showing the reads of Dvl1, Dvl2, and Dvl3 in mouse aortic SMC (n = 2 mice per group). RPKM: reads per kilobase per million mapped reads.

(D) Interaction between endogenous YAP and DVL3 in aortic SMC. Aortic SMC lysates were subjected to immunoprecipitation with an anti-YAP antibody. Elutes were analyzed by antibodies against DVL3 and YAP. Shown is one representative of three independent experiments.

Figure 4. *Continued*

(E) Western blot analysis of DVL3 in the aortic SMC lysates from control (Ctrl) and Sm-Yap/Taz-KO mice. The position of dephosphorylated (◀) and phosphorylated (◁) DVL3 is indicated. Shown is one representative of three independent experiments.

(F) Western blot analysis of DVL3 in the cytoplasmic and nuclear fraction of mouse aortic SMC two weeks after tamoxifen injection. The position of dephosphorylated (◀) and phosphorylated (◁) DVL3 is indicated. KO: Sm-Yap/Taz-KO. Lamin A/C was used as a nuclear marker and α-Tubulin as a cytoplasmic marker. s.e.: short exposure, l.e.: long exposure. Shown is one representative of three independent experiments.

(G) TOPflash reporter activity was measured in HEK293T cells transfected with an empty vector or plasmids expressing DVL3 or DVL3-NLS, which contains a nuclear localization sequence (NLS) (n = 4).

(H) TOPflash reporter activity was determined in human aortic smooth muscle cells (HASMCs) transfected with control siRNA or siRNA direct against Yap/Taz or the three Dvl isoforms.

(I) Western blot analysis of DVL3 in the cytoplasmic and nuclear fractions of HASMCs treated with control siRNA or siRNA directed against Yap/Taz. The bar diagram shows the densitometry analysis of nuclear DVL3 (n = 3).

(J) Quantitative RT-PCR analysis of the expression of the indicated genes in HASMC transfected with control siRNA or siRNA direct against Yap/Taz or the three Dvl isoforms (n = 4). Shown is one representative of three independent experiments.

Data are presented as mean ± SEM. *$p < 0.05$, **$p < 0.01$, and ***$p < 0.001$ (one-way ANOVA in G, H, and J, Student's t test in (I)).

different forms of vascular calcification (Cai et al., 2016; Cheng et al., 2014, 2015; Hortells et al., 2018; Shao et al., 2005; Voelkl et al., 2019). Several studies have described a positive regulation of Wnt signaling by YAP/TAZ (Heallen et al., 2011; Oudhoff et al., 2016; Rosenbluh et al., 2012), whereas YAP/TAZ have also been shown to suppress Wnt signaling by interaction with different components of the pathway (Azzolin et al., 2014; Barry et al., 2013; Imajo et al., 2012; Varelas et al., 2010). Our data clearly show that loss of YAP/TAZ in VSMCs results in increased expression of Wnt target genes but not in increased nuclear localization of β-catenin. Given that YAP/TAZ reside in the cytoplasm of VSMCs, we looked for cytoplasmatic interaction partners of YAP/TAZ and found DVL3, which interacts with YAP and is thereby prevented from mediating non-canonical Wnt signaling. Loss of YAP/TAZ is also accompanied by increase of DVL3 phosphorylation, which has been shown to promote nuclear translocation (Gan et al., 2008; Itoh et al., 2005; Wang et al., 2015). The mechanism mediating phosphorylation of DVL3 is unclear, but may involve casein kinase 1 δ/ϵ (Varelas et al., 2010). These findings are consistent with earlier data showing that TAZ can interact with DVL1, 2, and 3 in the cytoplasm, thereby inhibiting Wnt signaling (Varelas et al., 2010). Similarly, cytosolic YAP has been shown to inhibit DVL2 nuclear translocation to reduce Wnt downstream signaling independently of β-catenin (Barry et al., 2013).

YAP and TAZ have been shown to be involved in the differentiation of precursor cells into VSMCs during embryonic development. Loss of YAP/TAZ in premigratory neural crest cells results in vascular hemorrhages (Manderfield et al., 2014). Closer analysis revealed that YAP and TAZ are required for differentiation of neural crest precursors into VSMCs by physical and functional interaction with the Notch intracellular domain and subsequent activation of Notch target genes (Manderfield et al., 2015). Interestingly, Notch signaling has also been shown to suppress the chondrogenic differentiation of VSMCs during development as well as in the adult organism (Briot et al., 2014). This might suggest that YAP/TAZ suppress osteogenic differentiation by promoting Notch signaling. However, we did not find any evidence for reduced Notch signaling or Notch target gene activation in VSMCs of SM-Yap/Taz-KO mice.

The *in vivo* function of YAP in VSMCs has so far mainly been studied in the context of vascular injury, which has been shown to result in increased expression of YAP (Wang et al., 2012; Xie et al., 2012; Yu et al., 2019). This is consistent with *in vitro* studies in cultured VSMCs, which represent the proliferating state of smooth muscle cells and in which YAP/TAZ and the downstream transcription factor TEAD1 are activated (Feng et al., 2016; Liu et al., 2014; Wang et al., 2012; Xie et al., 2012). YAP and TEAD have been shown to suppress smooth muscle marker gene expression by inhibition of myocardin-dependent SRF transcriptional activity (Liu et al., 2014; Xie et al., 2012). Our data show that, under normal *in vivo* conditions, YAP and TAZ reside in the cytoplasm of VSMCs and do not exert transcriptional cofactor activity. However, through the retention of DVL in the cytoplasm, YAP and TAZ suppress Wnt signaling in VSMCs, thereby preventing osteogenic differentiation of VSMCs (Figure 5).

Thus, YAP and TAZ appear to have different functions depending on the activation state of VSMCs. After vascular injury, they translocate to the nucleus and repress smooth muscle-specific gene expression,

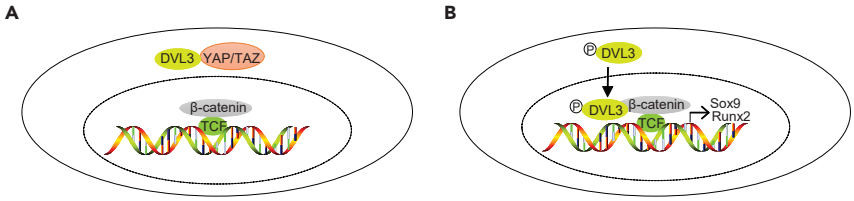

Figure 5. Schematic Diagram Summarizing the Proposed Function of YAP/TAZ in VSMC

(A) Under normal healthy conditions, YAP/TAZ sequester DVL3 in the cytosol of aortic SMCs.

(B) Loss of YAP/TAZ leads to the increase of DVL3 phosphorylation and nuclear translocation, resulting in the upregulation of osteogenic genes.

whereas, under normal healthy conditions, both cofactors stay in the cytoplasm to inhibit non-canonical Wnt signaling by sequestration of DVL and maintain the contractile phenotype of VSMCs.

Limitations of the Study

The present study demonstrated an important function of YAP/TAZ in maintenance of contractility of vascular smooth muscle cells *in vivo*. Loss of YAP/TAZ in vSMCs leads to reduced expression of smooth muscle marker genes, reduced contractility, and upregulation of osteogenic genes. Further studies are needed to examine the underlying mechanism of how loss of YAP/TAZ affects DVL3 phosphorylation and whether changes in YAP/TAZ expression or activity are responsible for the pathogenesis of vascular calcification in humans.

Resource Availability

Lead Contact

Further information and requests for resources and reagents should be directed to and will be fulfilled by the Lead Contact, Stefan Offermanns (stefan.offermanns@mpi-bn.mpg.de).

Materials Availability

This study did not generate any unique reagents.

Data and Code Availability

All the data are included in the manuscript and Supplemental Information. The RNA-seq data in this study are available at the National Center for Biotechnology Information's Gene Expression Omnibus database with accession numbers GSE146317 (https://www.ncbi.nlm.nih.gov/geo/query/acc.cgi?acc=GSE146317).

METHODS

All methods can be found in the accompanying Transparent Methods supplemental file.

SUPPLEMENTAL INFORMATION

Supplemental Information can be found online at https://doi.org/10.1016/j.isci.2020.101860.

ACKNOWLEDGMENTS

This study was supported by funds from the Max Planck Society. The authors wish to thank Svea Hümmer for excellent secretarial help and Dagmar Magalei, Kathrin Heil, Carola Meyer, and Nadine Rink for technical assistance. The authors would also like to thank Lin Li for sharing the Dvl3-NLS plasmid.

AUTHOR CONTRIBUTIONS

L.W. initiated and designed the study, performed most of the *in vitro* and *in vivo* experiments, analyzed data, and contributed to the writing of the manuscript; R.C., Y.-J.J., R.L., and S.P.W. helped with *in vitro* and *in vivo* experiments; S.G. and L.W. performed RNA sequencing and bioinformatics analysis; S.O.

initiated, designed, and supervised the study, discussed data, and wrote the manuscript. All authors commented on the manuscript.

DECLARATION OF INTERESTS

The authors declare no competing interests.

Received: May 11, 2020
Revised: September 10, 2020
Accepted: November 20, 2020
Published: December 18, 2020

REFERENCES

Abedin, M., Tintut, Y., and Demer, L.L. (2004). Vascular calcification: mechanisms and clinical ramifications. Arterioscler. Thromb. Vasc. Biol. *24*, 1161–1170.

Andrews, J., Psaltis, P.J., Bartolo, B.A.D., Nicholls, S.J., and Puri, R. (2018). Coronary arterial calcification: a review of mechanisms, promoters and imaging. Trends Cardiovasc. Med. *28*, 491–501.

Azzolin, L., Panciera, T., Soligo, S., Enzo, E., Bicciato, S., Dupont, S., Bresolin, S., Frasson, C., Basso, G., Guzzardo, V., et al. (2014). YAP/TAZ incorporation in the beta-catenin destruction complex orchestrates the Wnt response. Cell *158*, 157–170.

Barry, E.R., Morikawa, T., Butler, B.L., Shrestha, K., de la Rosa, R., Yan, K.S., Fuchs, C.S., Magness, S.T., Smits, R., Ogino, S., et al. (2013). Restriction of intestinal stem cell expansion and the regenerative response by YAP. Nature *493*, 106–110.

Bartoli-Leonard, F., Wilkinson, F.L., Langford-Smith, A.W.W., Alexander, M.Y., and Weston, R. (2018). The interplay of SIRT1 and Wnt signaling in vascular calcification. Front. Cardiovasc. Med. *5*, 183.

Bennett, M.R., Sinha, S., and Owens, G.K. (2016). Vascular smooth muscle cells in atherosclerosis. Circ. Res. *118*, 692–702.

Bostrom, K.I. (2000). Cell differentiation in vascular calcification. Z. Kardiol. *89*, 69–74.

Bostrom, K.I., Rajamannan, N.M., and Towler, D.A. (2011). The regulation of valvular and vascular sclerosis by osteogenic morphogens. Circ. Res. *109*, 564–577.

Briot, A., Jaroszewicz, A., Warren, C.M., Lu, J., Touma, M., Rudat, C., Hofmann, J.J., Airik, R., Weinmaster, G., Lyons, K., et al. (2014). Repression of Sox9 by Jag1 is continuously required to suppress the default chondrogenic fate of vascular smooth muscle cells. Dev. Cell *31*, 707–721.

Cai, T., Sun, D., Duan, Y., Wen, P., Dai, C., Yang, J., and He, W. (2016). WNT/beta-catenin signaling promotes VSMCs to osteogenic transdifferentiation and calcification through directly modulating Runx2 gene expression. Exp. Cell Res. *345*, 206–217.

Cheng, S.L., Behrmann, A., Shao, J.S., Ramachandran, B., Krchma, K., Bello Arredondo, Y., Kovacs, A., Mead, M., Maxson, R., and Towler, D.A. (2014). Targeted reduction of vascular Msx1 and Msx2 mitigates arteriosclerotic calcification and aortic stiffness in LDLR-deficient mice fed diabetogenic diets. Diabetes *63*, 4326–4337.

Cheng, S.L., Ramachandran, B., Behrmann, A., Shao, J.S., Mead, M., Smith, C., Krchma, K., Bello Arredondo, Y., Kovacs, A., Kapoor, K., et al. (2015). Vascular smooth muscle LRP6 limits arteriosclerotic calcification in diabetic LDLR-/- mice by restraining noncanonical Wnt signals. Circ. Res. *117*, 142–156.

Chow, B., and Rabkin, S.W. (2015). The relationship between arterial stiffness and heart failure with preserved ejection fraction: a systemic meta-analysis. Heart Fail. Rev. *20*, 291–303.

Daoud, F., Holmberg, J., Alajbegovic, A., Grossi, M., Rippe, C., Swärd, K., and Albinsson, S. (2020). Inducible deletion of YAP and TAZ in adult mouse smooth muscle causes rapid and lethal colonic pseudo-obstruction. Cell Mol. Gastroenterol. Hepatol. *28*, https://doi.org/10.1016/j.jcmgh.2020.09.014.

Demer, L.L., and Tintut, Y. (2008). Vascular calcification: pathobiology of a multifaceted disease. Circulation *117*, 2938–2948.

Durham, A.L., Speer, M.Y., Scatena, M., Giachelli, C.M., and Shanahan, C.M. (2018). Role of smooth muscle cells in vascular calcification: implications in atherosclerosis and arterial stiffness. Cardiovasc. Res. *114*, 590–600.

Feil, S., Fehrenbacher, B., Lukowski, R., Essmann, F., Schulze-Osthoff, K., Schaller, M., and Feil, R. (2014). Transdifferentiation of vascular smooth muscle cells to macrophage-like cells during atherogenesis. Circ. Res. *115*, 662–667.

Feng, X., Liu, P., Zhou, X., Li, M.T., Li, F.L., Wang, Z., Meng, Z., Sun, Y.P., Yu, Y., Xiong, Y., et al. (2016). Thromboxane A2 activates YAP/TAZ protein to induce vascular smooth muscle cell proliferation and migration. J. Biol. Chem. *291*, 18947–18958.

Gan, X.Q., Wang, J.Y., Xi, Y., Wu, Z.L., Li, Y.P., and Li, L. (2008). Nuclear Dvl, c-Jun, beta-catenin, and TCF form a complex leading to stabilization of beta-catenin-TCF interaction. J. Cell Biol. *180*, 1087–1100.

Gao, K., An, J., Zhang, Y., Jin, X., Ma, J., Peng, J., Tang, Y., Yu, L., Zhang, P., and Wang, C. (2015). The E3 ubiquitin ligase Itch and Yap1 have antagonistic roles in the regulation of ASPP2 protein stability. FEBS Lett. *589*, 94–101.

Gomez, D., and Owens, G.K. (2012). Smooth muscle cell phenotypic switching in atherosclerosis. Cardiovasc. Res. *95*, 156–164.

Heallen, T., Zhang, M., Wang, J., Bonilla-Claudio, M., Klysik, E., Johnson, R.L., and Martin, J.F. (2011). Hippo pathway inhibits Wnt signaling to restrain cardiomyocyte proliferation and heart size. Science *332*, 458–461.

Hortells, L., Sur, S., and St Hilaire, C. (2018). Cell phenotype transitions in cardiovascular calcification. Front. Cardiovasc. Med. *5*, 27.

Hruska, K.A., Mathew, S., and Saab, G. (2005). Bone morphogenetic proteins in vascular calcification. Circ. Res. *97*, 105–114.

Imajo, M., Miyatake, K., Iimura, A., Miyamoto, A., and Nishida, E. (2012). A molecular mechanism that links Hippo signalling to the inhibition of Wnt/beta-catenin signalling. EMBO J. *31*, 1109–1122.

Itoh, K., Brott, B.K., Bae, G.U., Ratcliffe, M.J., and Sokol, S.Y. (2005). Nuclear localization is required for Dishevelled function in Wnt/beta-catenin signaling. J. Biol. *4*, 3.

Jaminon, A., Reesink, K., Kroon, A., and Schurgers, L. (2019). The role of vascular smooth muscle cells in arterial remodeling: focus on calcification-related processes. Int. J. Mol. Sci. *20*, 5694.

Kawai-Kowase, K., and Owens, G.K. (2007). Multiple repressor pathways contribute to phenotypic switching of vascular smooth muscle cells. Am. J. Physiol. Cell Physiol. *292*, C59–C69.

Koo, J.H., and Guan, K.L. (2018). Interplay between YAP/TAZ and metabolism. Cell Metab. *28*, 196–206.

Lanzer, P., Boehm, M., Sorribas, V., Thiriet, M., Janzen, J., Zeller, T., St Hilaire, C., and Shanahan, C. (2014). Medial vascular calcification revisited: review and perspectives. Eur. Heart J. *35*, 1515–1525.

Lin, K.C., Park, H.W., and Guan, K.L. (2017). Regulation of the Hippo pathway transcription factor TEAD. Trends Biochem. Sci. *42*, 862–872.

Liu, F., Wang, X., Hu, G., Wang, Y., and Zhou, J. (2014). The transcription factor TEAD1 represses smooth muscle-specific gene expression by

abolishing myocardin function. J. Biol. Chem. *289*, 3308–3316.

Lu, J., Landerholm, T.E., Wei, J.S., Dong, X.R., Wu, S.P., Liu, X., Nagata, K., Inagaki, M., and Majesky, M.W. (2001). Coronary smooth muscle differentiation from proepicardial cells requires rhoA-mediated actin reorganization and p160 rho-kinase activity. Dev. Biol. *240*, 404–418.

Ma, S., Meng, Z., Chen, R., and Guan, K.L. (2019). The Hippo pathway: biology and pathophysiology. Annu. Rev. Biochem. *88*, 577–604.

Mack, C.P. (2011). Signaling mechanisms that regulate smooth muscle cell differentiation. Arterioscler. Thromb. Vasc. Biol. *31*, 1495–1505.

Mack, C.P., Somlyo, A.V., Hautmann, M., Somlyo, A.P., and Owens, G.K. (2001). Smooth muscle differentiation marker gene expression is regulated by RhoA-mediated actin polymerization. J. Biol. Chem. *276*, 341–347.

Manderfield, L.J., Aghajanian, H., Engleka, K.A., Lim, L.Y., Liu, F., Jain, R., Li, L., Olson, E.N., and Epstein, J.A. (2015). Hippo signaling is required for Notch-dependent smooth muscle differentiation of neural crest. Development *142*, 2962–2971.

Manderfield, L.J., Engleka, K.A., Aghajanian, H., Gupta, M., Yang, S., Li, L., Baggs, J.E., Hogenesch, J.B., Olson, E.N., and Epstein, J.A. (2014). Pax3 and Hippo signaling coordinate melanocyte gene expression in neural crest. Cell Rep. *9*, 1885–1895.

Miano, J.M. (2010). Vascular smooth muscle cell differentiation-2010. J. Biomed. Res. *24*, 169–180, Contractile properties of small arterial resistance vessels in spontaneously hypertensive and normotensive rats. Circ Res 41, 19-26.

Nakagawa, Y., Ikeda, K., Akakabe, Y., Koide, M., Uraoka, M., Yutaka, K.T., Kurimoto-Nakano, R., Takahashi, T., Matoba, S., Yamada, H., et al. (2010). Paracrine osteogenic signals via bone morphogenetic protein-2 accelerate the atherosclerotic intimal calcification in vivo. Arterioscler. Thromb. Vasc. Biol. *30*, 1908–1915.

Nicoll, R., and Henein, M.Y. (2014). The predictive value of arterial and valvular calcification for mortality and cardiovascular events. Int. J. Cardiol. Heart Vessel *3*, 1–5.

Olson, E.N., and Nordheim, A. (2010). Linking actin dynamics and gene transcription to drive cellular motile functions. Nat. Rev. Mol. Cell Biol. *11*, 353–365.

Oudhoff, M.J., Braam, M.J.S., Freeman, S.A., Wong, D., Rattray, D.G., Wang, J., Antignano, F., Snyder, K., Refaeli, I., Hughes, M.R., et al. (2016). SETD7 controls intestinal regeneration and tumorigenesis by regulating Wnt/beta-catenin and Hippo/YAP signaling. Dev. Cell *37*, 47–57.

Owens, G.K., Kumar, M.S., and Wamhoff, B.R. (2004). Molecular regulation of vascular smooth muscle cell differentiation in development and disease. Physiol. Rev. *84*, 767–801.

Paloian, N.J., and Giachelli, C.M. (2014). A current understanding of vascular calcification in CKD. Am. J. Physiol. Ren. Physiol. *307*, F891–F900.

Panciera, T., Azzolin, L., Cordenonsi, M., and Piccolo, S. (2017). Mechanobiology of YAP and TAZ in physiology and disease. Nat. Rev. Mol. Cell Biol. *18*, 758–770.

Posern, G., and Treisman, R. (2006). Actin' together: serum response factor, its cofactors and the link to signal transduction. Trends Cell Biol. *16*, 588–596.

Reginensi, A., Hoshi, M., Boualia, S.K., Bouchard, M., Jain, S., and McNeill, H. (2015). Yap and Taz are required for Ret-dependent urinary tract morphogenesis. Development *142*, 2696–2703.

Rong, J.X., Shapiro, M., Trogan, E., and Fisher, E.A. (2003). Transdifferentiation of mouse aortic smooth muscle cells to a macrophage-like state after cholesterol loading. Proc. Natl. Acad. Sci. U S A *100*, 13531–13536.

Rong, S., Zhao, X., Jin, X., Zhang, Z., Chen, L., Zhu, Y., and Yuan, W. (2014). Vascular calcification in chronic kidney disease is induced by bone morphogenetic protein-2 via a mechanism involving the Wnt/beta-catenin pathway. Cell Physiol. Biochem. *34*, 2049–2060.

Rosenbluh, J., Nijhawan, D., Cox, A.G., Li, X., Neal, J.T., Schafer, E.J., Zack, T.I., Wang, X., Tsherniak, A., Schinzel, A.C., et al. (2012). beta-Catenin-driven cancers require a YAP1 transcriptional complex for survival and tumorigenesis. Cell *151*, 1457–1473.

Sage, A.P., Tintut, Y., and Demer, L.L. (2010). Regulatory mechanisms in vascular calcification. Nat. Rev. Cardiol. *7*, 528–536.

Sakabe, M., Fan, J., Odaka, Y., Liu, N., Hassan, A., Duan, X., Stump, P., Byerly, L., Donaldson, M., Hao, J., et al. (2017). YAP/TAZ-CDC42 signaling regulates vascular tip cell migration. Proc. Natl. Acad. Sci. U S A *114*, 10918–10923.

Shalhoub, V., Shatzen, E., Henley, C., Boedigheimer, M., McNinch, J., Manoukian, R., Damore, M., Fitzpatrick, D., Haas, K., Twomey, B., et al. (2006). Calcification inhibitors and Wnt signaling proteins are implicated in bovine artery smooth muscle cell calcification in the presence of phosphate and vitamin D sterols. Calcif. Tissue Int. *79*, 431–442.

Shankman, L.S., Gomez, D., Cherepanova, O.A., Salmon, M., Alencar, G.F., Haskins, R.M., Swiatlowska, P., Newman, A.A., Greene, E.S., Straub, A.C., et al. (2015). KLF4-dependent phenotypic modulation of smooth muscle cells has a key role in atherosclerotic plaque pathogenesis. Nat. Med. *21*, 628–637.

Shao, J.S., Cheng, S.L., Pingsterhaus, J.M., Charlton-Kachigian, N., Loewy, A.P., and Towler, D.A. (2005). Msx2 promotes cardiovascular calcification by activating paracrine Wnt signals. J. Clin. Invest. *115*, 1210–1220.

Shimizu, T., Tanaka, T., Iso, T., Doi, H., Sato, H., Kawai-Kowase, K., Arai, M., and Kurabayashi, M. (2009). Notch signaling induces osteogenic differentiation and mineralization of vascular smooth muscle cells: role of Msx2 gene induction via Notch-RBP-Jk signaling. Arterioscler. Thromb. Vasc. Biol. *29*, 1104–1111.

Sobue, K., Hayashi, K., and Nishida, W. (1999). Expressional regulation of smooth muscle cell-specific genes in association with phenotypic modulation. Mol. Cell Biochem. *190*, 105–118.

Speer, M.Y., Yang, H.Y., Brabb, T., Leaf, E., Look, A., Lin, W.L., Frutkin, A., Dichek, D., and Giachelli, C.M. (2009). Smooth muscle cells give rise to osteochondrogenic precursors and chondrocytes in calcifying arteries. Circ. Res. *104*, 733–741.

Takahashi, M., Hayashi, K., Yoshida, K., Ohkawa, Y., Komurasaki, T., Kitabatake, A., Ogawa, A., Nishida, W., Yano, M., Monden, M., et al. (2003). Epiregulin as a major autocrine/paracrine factor released from ERK- and p38MAPK-activated vascular smooth muscle cells. Circulation *108*, 2524–2529.

Totaro, A., Panciera, T., and Piccolo, S. (2018). YAP/TAZ upstream signals and downstream responses. Nat. Cell Biol. *20*, 888–899.

Varelas, X., Miller, B.W., Sopko, R., Song, S., Gregorieff, A., Fellouse, F.A., Sakuma, R., Pawson, T., Hunziker, W., McNeill, H., et al. (2010). The Hippo pathway regulates Wnt/beta-catenin signaling. Dev. Cell *18*, 579–591.

Vattikuti, R., and Towler, D.A. (2004). Osteogenic regulation of vascular calcification: an early perspective. Am. J. Physiol. Endocrinol. Metab. *286*, E686–E696.

Vengrenyuk, Y., Nishi, H., Long, X., Ouimet, M., Savji, N., Martinez, F.O., Cassella, C.P., Moore, K.J., Ramsey, S.A., Miano, J.M., et al. (2015). Cholesterol loading reprograms the microRNA-143/145-myocardin axis to convert aortic smooth muscle cells to a dysfunctional macrophage-like phenotype. Arterioscler. Thromb. Vasc. Biol. *35*, 535–546.

Voelkl, J., Lang, F., Eckardt, K.U., Amann, K., Kuro, O.M., Pasch, A., Pieske, B., and Alesutan, I. (2019). Signaling pathways involved in vascular smooth muscle cell calcification during hyperphosphatemia. Cell. Mol. Life Sci. *76*, 2077–2091.

Voelkl, J., Luong, T.T., Tuffaha, R., Musculus, K., Auer, T., Lian, X., Daniel, C., Zickler, D., Boehme, B., Sacherer, M., et al. (2018). SGK1 induces vascular smooth muscle cell calcification through NF-kappaB signaling. J. Clin. Invest. *128*, 3024–3040.

Wang, X., Hu, G., Gao, X., Wang, Y., Zhang, W., Harmon, E.Y., Zhi, X., Xu, Z., Lennartz, M.R., Barroso, M., et al. (2012). The induction of Yes-associated protein expression after arterial injury is crucial for smooth muscle phenotypic modulation and neointima formation. Arterioscler. Thromb. Vasc. Biol. *32*, 2662–2669.

Wang, W., Li, X., Lee, M., Jun, S., Aziz, K.E., Feng, L., Tran, M.K., Li, N., McCrea, P.D., Park, J.I., et al. (2015). FOXKs promote Wnt/beta-catenin signaling by translocating DVL into the nucleus. Dev. Cell *32*, 707–718.

Wang, Z., Wang, D.Z., Hockemeyer, D., McAnally, J., Nordheim, A., and Olson, E.N. (2004). Myocardin and ternary complex factors compete for SRF to control smooth muscle gene expression. Nature *428*, 185–189.

Wirth, A., Benyo, Z., Lukasova, M., Leutgeb, B., Wettschureck, N., Gorbey, S., Orsy, P., Horvath, B., Maser-Gluth, C., Greiner, E., et al. (2008). G12-G13-LARG-mediated signaling in vascular

smooth muscle is required for salt-induced hypertension. Nat. Med. *14*, 64–68.

Woldt, E., Terrand, J., Mlih, M., Matz, R.L., Bruban, V., Coudane, F., Foppolo, S., El Asmar, Z., Chollet, M.E., Ninio, E., et al. (2012). The nuclear hormone receptor PPARgamma counteracts vascular calcification by inhibiting Wnt5a signalling in vascular smooth muscle cells. Nat. Commun. *3*, 1077.

Xie, C., Guo, Y., Zhu, T., Zhang, J., Ma, P.X., and Chen, Y.E. (2012). Yap1 protein regulates vascular smooth muscle cell phenotypic switch by interaction with myocardin. J. Biol. Chem. *287*, 14598–14605.

Xin, M., Kim, Y., Sutherland, L.B., Murakami, M., Qi, X., McAnally, J., Porrello, E.R., Mahmoud, A.I., Tan, W., Shelton, J.M., et al. (2013). Hippo pathway effector Yap promotes cardiac regeneration. Proc. Natl. Acad. Sci. U S A *110*, 13839–13844.

Yahagi, K., Kolodgie, F.D., Lutter, C., Mori, H., Romero, M.E., Finn, A.V., and Virmani, R. (2017). Pathology of Human coronary and carotid artery atherosclerosis and vascular calcification in diabetes mellitus. Arterioscler. Thromb. Vasc. Biol. *37*, 191–204.

Yao, L., Sun, Y.T., Sun, W., Xu, T.H., Ren, C., Fan, X., Sun, L., Liu, L.L., Feng, J.M., Ma, J.F., et al. (2015). High phosphorus level leads to aortic calcification via beta-catenin in chronic kidney disease. Am. J. Nephrol. *41*, 28–36.

Yoshida, T., Yamashita, M., Horimai, C., and Hayashi, M. (2017). Smooth muscle-selective Nuclear Factor-kappaB inhibition reduces phosphate-induced arterial medial calcification in mice with chronic kidney disease. J. Am. Heart Assoc. *6*, e007248.

Yu, Q., Li, W., Jin, R., Yu, S., Xie, D., Zheng, X., Zhong, W., Cheng, X., Hu, S., Li, M., et al. (2019). PI3Kgamma (Phosphoinositide 3-Kinase gamma) regulates vascular smooth muscle cell phenotypic modulation and neointimal formation through CREB (cyclic AMP-response element binding protein)/YAP (Yes-associated protein) signaling. Arterioscler. Thromb. Vasc. Biol. *39*, e91–e105.

Zhao, G., Xu, M.J., Zhao, M.M., Dai, X.Y., Kong, W., Wilson, G.M., Guan, Y., Wang, C.Y., and Wang, X. (2012). Activation of nuclear factor-kappa B accelerates vascular calcification by inhibiting ankylosis protein homolog expression. Kidney Int. *82*, 34–44.

Zheng, Y., and Pan, D. (2019). The Hippo signaling pathway in development and disease. Dev. Cell *50*, 264–282.

Zhu, D., Mackenzie, N.C., Shanahan, C.M., Shroff, R.C., Farquharson, C., and MacRae, V.E. (2015). BMP-9 regulates the osteoblastic differentiation and calcification of vascular smooth muscle cells through an ALK1 mediated pathway. J. Cell Mol. Med. *19*, 165–174.

iScience, Volume *23*

Supplemental Information

YAP/TAZ Are Required to Suppress Osteogenic Differentiation of Vascular Smooth Muscle Cells

Lei Wang, Ramesh Chennupati, Young-June Jin, Rui Li, ShengPeng Wang, Stefan Günther, and Stefan Offermanns

Supplemental Figures and Legends

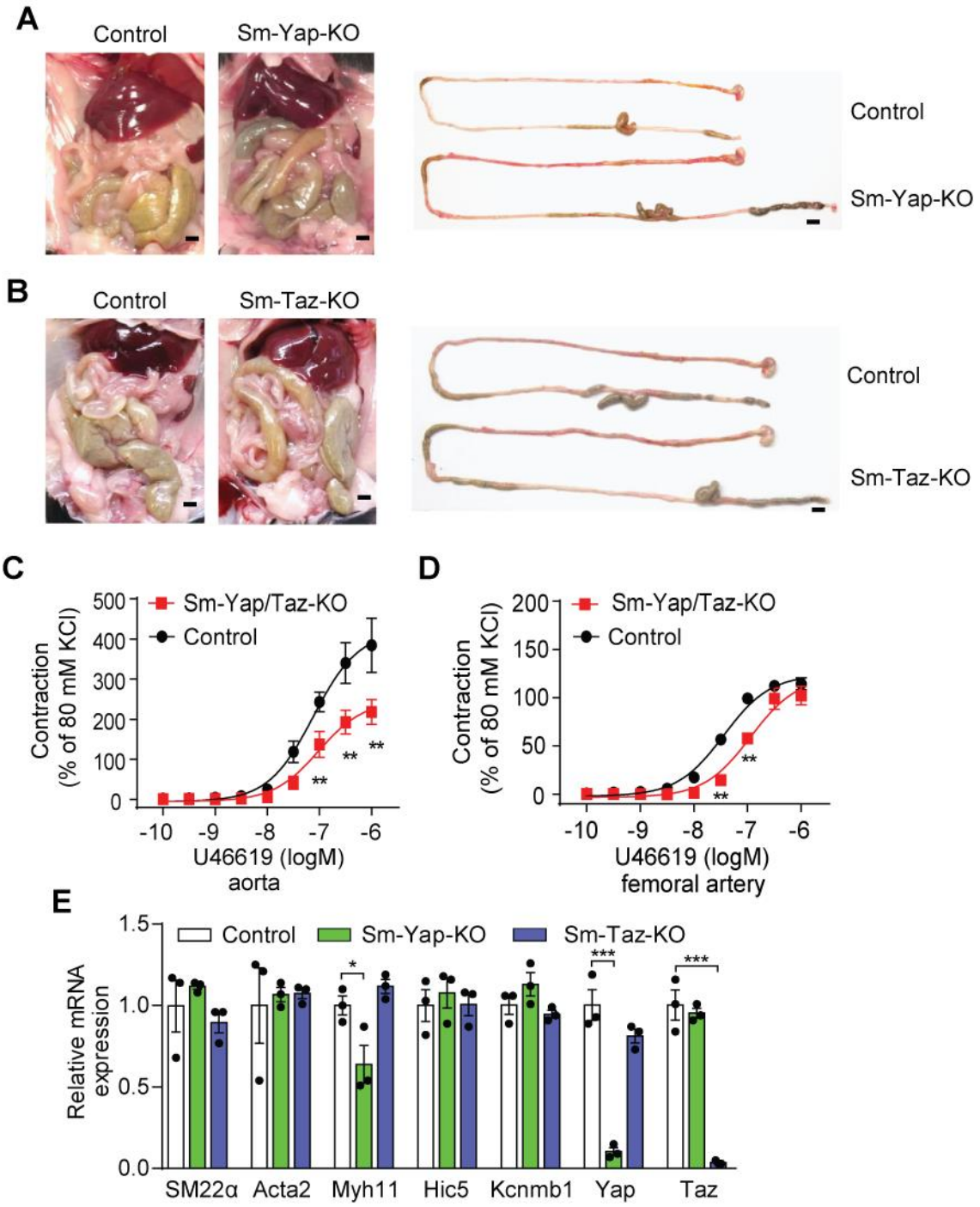

Figure S1. Single Yap or Taz deficiency in aorta SMC does not affect the differentiated phenotype, Related to Figure 1. (A, B) Macroscopic analysis of the gastrointestinal tracts of Sm-Yap-KO mice (A) and Sm-Taz-KO mice (B). Scale bar: 1 cm. **(C, D)** The contractile response to the thromboxane A_2 analogue U46619 of thoracic aortae (C, n = 3 mice per group) and femoral arteries (D, n = 3 mice per group). **(E)** Quantitative RT-PCR *showing the* smooth muscle marker gene expression in the aortic SMCs of Sm-Yap-KO or Sm-Taz-KO mice two weeks after the last tamoxifen injection (n = 3 mice per group). In C-E one representative experiment of two independent experiments is shown. Data are presented as mean ± SEM. *$p < 0.05$, **$p < 0.01$ and ***$p < 0.001$ (Two-way ANOVA in **C** and **D**, and One-way ANOVA in **E**).

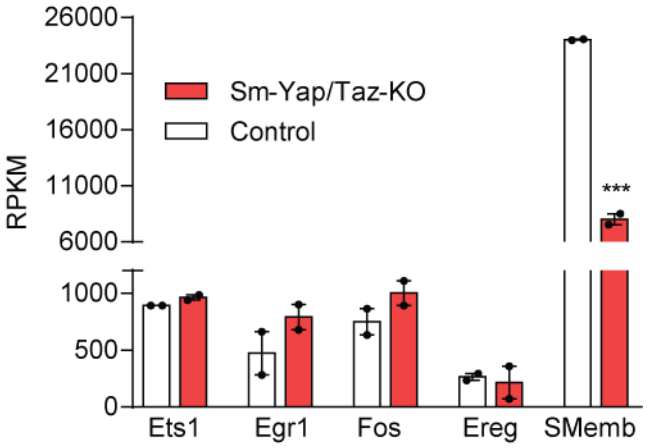

Figure S2. Expression of early response genes and the synthetic VSMC phenotype marker gene SMemb in mouse aortic SMCs of control and Sm-Yap/Taz-KO mice, Related to Figure 2. Expression was determined by RNA-seq. (n = 2 mice per group). RPKM: reads per kilobase per million mapped reads. Data are presented as mean ± SEM.

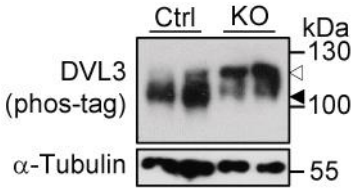

Figure S3. Analysis of DVL3 mobility shift in the aortic SMCs lysates from control (Ctrl) and Sm-Yap/Taz-KO (KO) mice on a phos-tag gel, Related to Figure 4. Upper arrowhead (◁) indicates phosphorylated Dvl3. Lower arrowhead (◄) corresponds to the dephosphorylated DVL on a phos-tag gel.

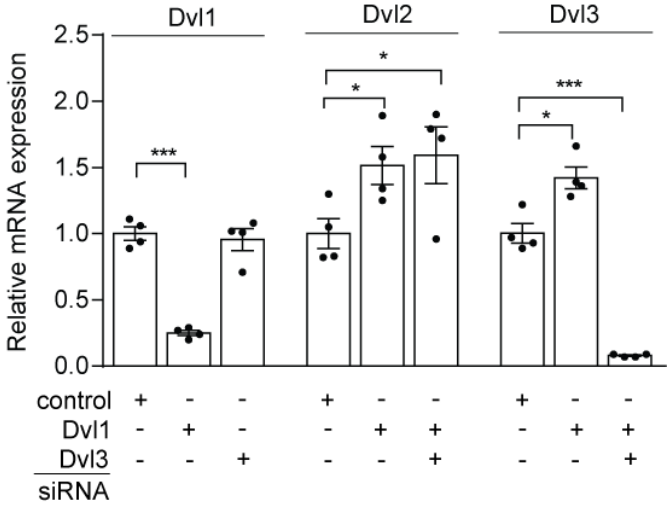

Figure S4. Quantitative RT-PCR analysis of expression of DVL isoforms after knockdown of Dvl1 or Dvl3 in human aortic smooth muscle cells (HASMC), Related to Figure 4. Data are presented as mean ± SEM. *$p < 0.05$, ***$p < 0.001$ (One-way ANOVA).

Transparent Methods

Animals.

The generation of floxed alleles of the genes encoding Yap and Taz (Wwtr1) has been described previously (Wang, et al. 2020). All mouse lines were on a C57/BL6 background. Smooth muscle-specific Yap/Taz deficient mice (Sm-Yap/Taz-KO) were generated by crossing $Yap^{fl/fl}$; $Taz^{fl/fl}$ mice with Myh11-$CreER^{T2}$ transgenic mice (Wirth et al., 2008). Since Myh11-$CreER^{T2}$ transgenic mice carry the transgene on the Y chromosome, all experiments were performed in males. For induction of Cre-mediated recombination in Sm-Yap/Taz-KO mice, 1 mg of tamoxifen was injected intraperitoneally for 5 consecutive days at the age of 8-12 weeks old. Tamoxifen-treated $Yap^{fl/fl}$;$Taz^{fl/fl}$ age-matched male mice served as controls. Animals were fed a standard diet (SD, Altromin) with water ad libitum. All procedures of animal care and use in this study were approved by the local animal welfare authorities and committees (Regierungspräsidia Karlsruhe and Darmstadt).

Cell culture and transfection. Human aortic smooth muscle cells (HASMCs) were purchased from Lonza (#CC-2571) and were cultured in smooth muscle cell growth medium (Lonza, SmBM, #CC-3181) supplemented with 5% FBS, 0.1% insulin, 0.2% basic human fibroblast growth factor (hFGF-b), 0.1% GA-100, and 0.1% human epidermal growth factor (hEGF) (Lonza, #CC-4149). HASMCs were transfected with the TOPflash reporter plasmid (Addgene, #12456) and a constitutively expressing Renilla luciferase plasmid with Basic Nucleofector™ Kit for Primary Mammalian Smooth Muscle Cells (Lonza, Catalog #VPI-1004). HEK293T cells were maintained in DMEM supplemented with 10% FBS, 1% penicillin and streptomycin, 1% L-glutamine and 1% sodium pyruvate. Cells were maintained at 37°C in a humidified atmosphere with 5% CO_2. HEK293T cells were transfected with the TOPflash reporter plasmid (Addgene, #12456) and a constitutively expressing Renilla luciferase plasmid as well as the tested plasmids Flag-DVL3 (Addgene, #16758) or Dvl3-NLS (Gan et al., 2008) using Lipofectamine 2000 (Invitrogen). Cells were lysed, and firefly luciferase activity was determined using the Dual-Luciferase(R) Reporter Assay System (Promega, E1910) 48 h after transfection. Firefly luciferase activity was normalized by measuring the expression of Renilla luciferase and background activity was subtracted.

siRNA-mediated knock-down. HASMCs cells were transfected with siRNA using Lipofectamine RNAiMax transfection reagent (Invitrogen) according to the manufacturer's instructions. The targeted sequences of human siRNAs directed against RNAs encoding Yap, Taz, Dvl1, Dvl2 and Dvl3 were: Yap, 5′-CAGGTGATACTATCAACCAAA-3′; Taz, 5′-CTGCGTTCTTGTGACAGATTA-3′; Dvl1, 5′-GCGACATGTTGCTGCAGGT-3′, Dvl2, 5′-CTAGTCAACCTGTCTCTCA-3′, Dvl3 5′-GATATGTTGTTACAGGTAA-3′.

Wire myography. Two weeks after the last tamoxifen injection, thoracic aortae, fermoral ateries or first order mesenteric arteries (2 mm length) were removed from the mesentery and were mounted on a conventional myograph setup (610-M, Danish Myo Technology) and kept in 5 ml Krebs solution maintained at 37°C and aerated with 95% O_2/5% CO_2. Aorta and femoral arteries were progressively stretched until a diameter corresponding to 90% of the passive diameter at a transmural pressure of 100 mmHg (Mulvany and Halpern, 1977). Whereas mesenteric arterial segments were distended to the

diameter at which maximal contractile responses to 10 µM noradrenaline were observed (Meens et al., 2012). All arterial segments were allowed for 30 min to recover after normalization. Endothelial integrity was checked, the segments which show lower than 80% relaxation were discarded from the experiment. The contractile responses to the indicated agonists were tested as described (Wirth et al., 2008). Between each agonist dose-response curve, a 20 min recovery time was maintained.

Immunofluorescence staining. Mice were perfused with PBS and fixed in 4% paraformaldehyde for the preparation of frozen sections. Sections were permeabilized in 0.1% Triton/PBS (PBS-T) for 5 minutes, followed by 3 times washes in PBS. Sections were incubated in blocking buffer (1% BSA in PBS-T) for 1 hour at room temperature and then incubated overnight at 4 °C with the primary antibody indicated in the blocking buffer. The antibodies for immunostaining included: β-catenin (BD Bioscience, #610154), YAP/TAZ (Cell signaling Technology, #2149), SM α-Actin (Sigma, FITC-conjugated, F3777). Sections were washed 3 times in PBS and then incubated with a secondary antibody for 1 h at room temperature. Donkey anti-mouse Alexa Fluor 594, or donkey anti-rabbit Alexa Fluor 594 secondary antibodies (Life Technologies, Thermo Fisher Scientific) were used. Sections were washed 3 times in PBS-T and then mounted with mounting medium with DAPI. Immunofluorescence imaging was performed using a Leica laser scanning microscope.

Von Kossa staining, Alkaline phosphate (ALPL) activity assay and Calcium content measurement. For Von Kossa staining, aorta paraffin sections were dewaxed, dehydrated and incubated in 1% silver nitrate (Sigma) under UV light for 1 h. Then the slides were washed twice in distilled H_2O and immersed in 5% sodium thiosulfate for 5 min, followed by counterstain with nuclear fast red for 5 minutes. Alkaline phosphatase (ALPL) activity was determined following the instructions of an alkaline phosphatase activity colorimetric assay kit (BioVision, K412). U/g: Unit (U) per gram aorta tissue. Unit (U) represents the amount of ALPL enzyme causing the hydrolysis of one micromole of *p*NPP (*p*-nitrophenyl phosphate) per minute at pH 9.6 and 25 ^{o}C. Calcium content measurement was performed according to the instructions of calcium colorimetric assay kit (Sigma, MAK022). Briefly, aortae were incubated with 1 M HCl at 37 °C for 18 h (Sheen et al., 2015). Calcium concentration in the solution was determined by measuring the concentration of the o-cresolphthalein complex at 575 nm. Aortae were dried at 55 °C for 18 h, and then weighed. The amount of aortic calcium content was normalized to tissue dry weight and expressed as µg calcium per mg aorta dry weight.

Quantitative RT-PCR and RNA-seq. Total RNA was isolated from aortic SMCs using the RNeasy Micro Kit (Qiagen, Valencia, CA, USA), and DNA was removed using the QIAGEN RNase-Free DNase Set following the manufacturer's instructions. cDNA was synthesized using ProtoScript® II reverse transcriptase (New England Biolabs). Quantitative RT-PCR was performed using LightCycler 480 Real-Time PCR detection System (Roche Molecular Biochemicals, Mannheim, Germany) according to the manufacturer's instructions. Relative mRNA expression was determined by the ΔCt method. The expression results were normalized to GAPDH. Data are presented as relative values and gene expression in controls was set to 1. For the following primers were used to analyze mRNA expression: SM22α (probe #5) forward 5'-GCAGTGTGGCCCTGATGTA-3', reverse 5'-TCACCAATTTGCTCAGAATCA-3'; Acta2 (probe #58) forward 5'-CCAGCACCATGAAGATCAAG-3', reverse 5'-TGGAAGGTAGACAGCGAAGC-3'; Myh11 (probe #68) forward 5'-

TGGAGGCCAAGATTGCAC-3', reverse 5'-GGCCGCCTGTTTCTCTCT-3'; Cnn1 (probe #15) forward 5'-CGGCTTGTCTGCTGAAGTAA-3', reverse 5'-ACCCCCTCAATCCACTCTCT-3'; Hic-5 (probe #16) forward 5'-AATAAACCTATAGCTGGGCAAGTG-3', reverse 5'-AAAAGGGAGCCCCATCCT-3'; Kcnmb1 (probe #60) forward 5'-GCGGAGACCCAGAGAACTAAA-3', reverse 5'-CTTCTGGGCCATCACCAG-3'; Yap (probe #40) forward 5'-CCTTTGAGATCCCTGATGATG-3', reverse 5'-GCCATGTTGTTGTCTGATCG-3'; Taz (probe #110) forward 5'-GCCACTGGCCAGAGATACTT-3', reverse 5'-GACGGGTGGAGGTTCACAT-3'; Runx2 (probe #99) forward 5'-GCACCGACAGTCCCAACT-3', reverse 5'-CCTCTCCGAGGGCTACAAC-3'; Alpl (probe #12) forward 5'-CGGATCCTGACCAAAAACC-3', reverse 5'-TCATGATGTCCGTGGTCAAT-3'; Spp1 (probe #52) forward 5'-TTGGCAGTGATTTGCTTTTG-3', reverse 5'-TCTGGGTGCAGGCTGTAAA-3'; Col1a1 (probe #15) forward 5'-AGACATGTTCAGCTTTGTGGAC-3', reverse 5'-CAGCTGACTTCAGGGATG-3'; Cd44 (probe #29) forward 5'-GCATCGCGGTCAATAGTAGG-3', reverse 5'-CACCGTTGATCACCAGCTT-3'; Ephb2 (probe #9) forward 5'-TCACCTCAGTTCGCCTCTG-3', reverse 5'-TCACCTGGTGCATGATGG-3'; Sox9 (probe #66) forward 5'-GTACCCGCATCTGCACAAC-3', reverse 5'-CTCCTCCACGAAGGGTCTCT-3'; Wisp1 (probe #92) forward 5'-GCTGACTTCCAGGCATGAG-3', reverse 5'-GTTGTGGGGGTTGGAGAGA-3'; Ccnd1 (probe #72) forward 5'-TTCTTTCCAGAGTCATCAAGTGT-3', reverse 5'-TGACTCCAGAAGGGCTTCAA-3'.

RNA-seq was performed as described previously (Wang, et al. 2020). The list of differentially expressed genes is provided in Supplemental Table 1. The RNA-Seq data have been deposited in NCBI under the accession number GSE146317.

Immunoprecipitation and Western blotting. For immunoprecipitation of endogenous YAP and DVL3, mouse aortae were homogenized with the lysis buffer (Li et al., 1999) containing 1% NP-40, 137 mM sodium chloride, 20 mM Tris-HCl, pH 7.4, 1 mM dithiothreitol, 10% glycerol, 10 mM sodium fluoride, 1 mM pyrophosphate, 2 mM sodium vanadate and protease inhibitor. The lysates were incubated with a rabbit anti-YAP antibody (Cell Signaling Technology, #4912, 1:100) or a control rabbit IgG (Cell Signaling Technology, #2729) and protein A/G–Sepharose beads (Santa Cruz Biotech, CA, #sc-2003). The immunocomplexes were pelleted and washed with lysis buffer 3 times. The precipitated proteins were released by boiling in an SDS sample buffer. For mouse aortic SMC protein extraction, samples were homogenized using Retsch MM 300 Tissue Lyser Mixer Mill in RIPA buffer (10 mM Tris-HCl pH 8.0, 1 mM EDTA, 1% Triton X-100, 0.1% SDS, 0.1% sodium deoxycholate, 140 mM sodium chloride, phosphatase and protease inhibitors). Extracts were spun down, and supernatants were collected. The nuclear *and* cytoplasmic fractionation was performed according to the instructions of NE-PER™ Nuclear and Cytoplasmic Extraction Reagents (Thermo Scientific, #7833). Human aortic smooth muscle cells (HASMCs) were treated with control siRNA or siRNA directed against Yap/Taz followed by serum-free starvation for 48 h as well as with 5 ng/ml leptomycin B for 4 h, then collected for cellular fractionation. Immunoprecipitates, total cell lysates or cellular fractionations of protein lysates were loaded on SDS-PAGE gels and were analyzed by immunoblotting with the indicated antibodies. For detection, Pierce™ ECL Western Blotting Substrate (Thermo Scientific) or Immobilon Western Chemiluminescent HRP Substrate (Merck) was used. The following antibodies were obtained from Cell Signaling Technology: anti-YAP/TAZ (#8418, 1:1,000), anti-Lamin A/C (#2032, 1:1,000), anti-GAPDH (#2118, 1:3,000), anti-P65 (#4764, 1:1,000), anti-phospho-P65 (Ser536) (#3033, 1:1,000), anti-phospho-

SMAD2(Ser465/467)/SMAD3(Ser423/425) (#8828, 1:1,000), anti-DVL3 (#3218, 1:1,000), anti-NOTCH2 (#5732, 1:1,000). Anti-ACTA2 (#ab5694, 1:2,000), anti-SM22α (#ab14106, 1:2,000) and anti-MYH11 (#ab53219, 1:2,000) antibodies were obtained from Abcam. Anti-β-catenin (#610154, 1:1,000) was obtained from BD Bioscience. Anti-α-Tubulin (#T9026, 1:3,000) was from Sigma-Aldrich and anti-ALPL (#AF2910, 1:1,000) was obtained from R&D System. Anti-mouse and rabbit HRP-conjugated secondary antibodies were from Cell Signaling Technology. Anti-goat and anti-rat HRP-conjugated secondary antibodies were from Santa Cruz Biotechnology.

Statistics. Data are expressed as mean ± SEM. Comparisons between groups were performed with unpaired two-tailed Student's *t*-test or ANOVA. A p value less than or equal to 0.05 was considered significant (*$p < 0.05$; **$p < 0.01$; ***$p < 0.001$). Statistical analysis was performed with Prism5 or Prism6 (GraphPad) or Excel (Microscoft) software.

Supplemental References

Li, L., Yuan, H., Weaver, C.D., Mao, J., Farr, G.H., 3rd, Sussman, D.J., Jonkers, J., Kimelman, D., and Wu, D. (1999). Axin and Frat1 interact with dvl and GSK, bridging Dvl to GSK in Wnt-mediated regulation of LEF-1. EMBO J. *18*, 4233-4240.

Meens, M.J., Mattheij, N.J., van Loenen, P.B., Spijkers, L.J., Lemkens, P., Nelissen, J., Compeer, M.G., Alewijnse, A.E., and De Mey, J.G. (2012). G-protein betagamma subunits in vasorelaxing and anti-endothelinergic effects of calcitonin gene-related peptide. Br. J. Pharmacol. *166*, 297-308.

Mulvany, M. J. and W. Halpern (1977). "Contractile properties of small arterial resistance vessels in spontaneously hypertensive and normotensive rats." Circ. Res. *41(1)*: 19-26.

Sheen, C.R., Kuss, P., Narisawa, S., Yadav, M.C., Nigro, J., Wang, W., Chhea, T.N., Sergienko, E.A., Kapoor, K., Jackson, M.R.*, et al.* (2015). Pathophysiological role of vascular smooth muscle alkaline phosphatase in medial artery calcification. J. Bone Miner. Res. *30*, 824-836.

Wang, L., S. Wang, Y. Shi, R. Li, S. Günther, Y. T. Ong, M. Potente, Z. Yuan, E. Liu and S. Offermanns (2020). YAP and TAZ protect against white adipocyte cell death during obesity. Nat. Commun. *11,* 5455.

Wirth, A., Benyo, Z., Lukasova, M., Leutgeb, B., Wettschureck, N., Gorbey, S., Orsy, P., Horvath, B., Maser-Gluth, C., Greiner, E.*, et al.* (2008). G12-G13-LARG-mediated signaling in vascular smooth muscle is required for salt-induced hypertension. Nat. Med. *14*, 64-68.